# Examination of Fracture Mechanisms in two Al – Ti – V – Cr – (Si) High Entropy Alloys

*Spyridon* Chaskis[1*], *Dimitrios* Kiousis[1], *Pavlos* Stavroulakis[2], *Russell* Goodall[2], *Spyros* Papaefthymiou[1]

[1]Laboratory of Physical Metallurgy, Division of Metallurgy and Materials, School of Mining and Metallurgical Engineering, National Technical University of Athens, 9, Her. Polytechniou Str., Zografos, 15780 Athens, Greece
[2]Department of Material Science & Engineering, The University of Sheffield, Sir Robert Hadfield Building, Mappin St, Sheffield, S13 JD, United Kingdom

**Abstract.** This work focuses on the examination of two High Entropy Alloys (HEAs), the AlTiVCr and AlTiVCr–$Si_{7.2}$, which have been observed to fail in a brittle manner directly after casting. Understanding the failure mechanics is a prerequisite for an alternative enhanced alloy design in order to prevent early failure without loading application. The specimens were produced using the Vacuum Arc Melting methodology in a protective argon atmosphere. The material was re–melted five times in combination with electromagnetic stirring in order to achieve a fully homogenized microstructure. Based on our findings, the failure occurred in the first 10 minutes after casting during slow cooling. Similarly, the same took place during thermal treatment after the third re–melting. The specimens were first prepared for optical (OM) and scanning electron microscopy (SEM) analysis. The material consists of a coarse dendritic microstructure as well as a retained BCC phase, which is the AlTiVCr phase. In the AlTiVCr – $Si_{7.2}$ alloy a uniformly dispersed, angular intermetallic compound, namely the $Ti_5Si_3$, was identified, which increases the failure resistance of the material. Based on these findings the alloy will be redesigned.

## 1 Introduction

This study involves two High-Entropy alloys (HEAs), namely one is Al-Ti-V-Cr and the other one is the one with addition of 7.2 at. % Silicon that have been observed to fail in a brittle way after casting. There are 2 widely accepted approaches used in order to define what a HEA is. The first one categorizes HEAs as alloys, which contain at least 5 main alloying elements varying from 5 to 35 at. % and potential additional elements below 5 at. %. The second approach is based on the configurational entropy and accepts HEAs as alloys which have:

$$\Delta S_{conf} > 1.5R \quad (1)$$

Where: ΔSconf. = configurational entropy.

* Corresponding author: s.chaskis@metal.ntua.gr

$$\Delta S_{conf} = -R\sum_{i=1}^{n} c_i \ln(c_i) \quad (2)$$

Where: R = 8.314 J/K mol (gas constant)
ci = atomic concentration of element i [1].

The alloys produced in this study can be considered as Medium-Entropy Alloys (MEAs)

$$1R \leq \Delta S_{conf} \leq 1.5R \quad (3)$$

Although, in the existing literature it is mentioned as HEA [2][3]. This alloy is a polycrystalline single-phase alloy with a body-centered cubic (BCC) solid solution structure. In BCC systems the most common structures are BCC_A2 and BCC_B2. Where A2 refers to disordered BCC, while B2 to ordered (semi-ordered) BCC [4][5][6]. Thermodynamical calculations (TCHEA2) reveal the possibility of a transformation, which is called as "order-disorder" transformation and it seems to occur at 700 °C (973K), as reported in X. Huang et. al. research work [7]. Above 700 °C, the existing parent phase is BCC_A2, while below 700 °C, it is transformed into BCC_B2. By adding Silicon at 5 at. %, formation of a secondary $Ti_5Si_3$ phase is achieved [7].

The microalloyed Al-Ti-V-Cr-$Si_5$ alloy's matrix still has BCC structure and based on CALPHAD calculations, the possibility of BCC_A2 to BCC_B2 phase transformation occurring during cooling. It is noted that microalloying affects "order-disorder" transformation temperature and induces an increase in hardness [7]. Typical structure of BCC_A2 and BCC_B2 can be seen below in Fig. 1. In addition, alloy's total density is reduced [7]. Based on the degree of ordering, alloys macroscopic properties are affected as well. During A2 → B2 transformation, decrease of ductility and enhance of yield strength is reported. Additionally, in HEAs with BCC_B2, when the range of ordering decreases, the alloy's total ductility of increases [8].

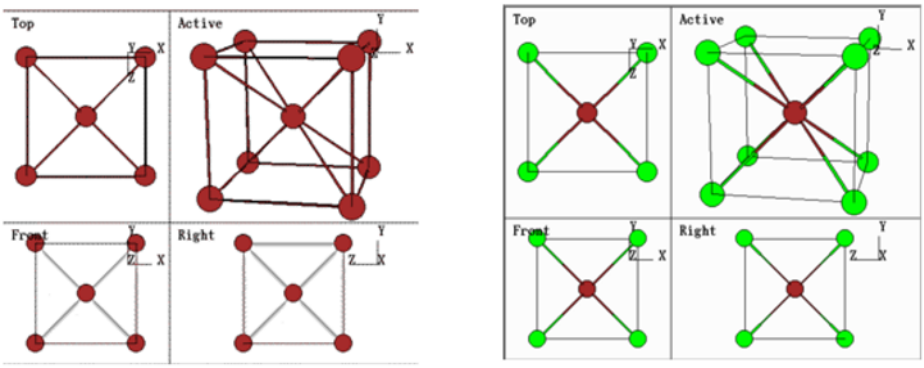


Fig. 1: Structure of A2 and B2 body-centered cubic (BCC) systems [9], [10].

Understanding the failure mechanisms is a prerequisite for an alternative enhanced alloy design in order to prevent early failure without loading application. Thus, the scope of this project is to provide a first insight to failure mechanisms and in that way to acquire information to further modify the casting process or these alloys and prevent any future potential failure.

## 2 Experimental Approach

Two alloys are produced utilizing the Vacuum Arc Melting (VAR) technique and both were re-melted 4-5 times in combination with electromagnetic stirring, in order to achieve a fully homogenized microstructure. One is the Al-Ti-V-Cr and the latter is the microalloyed Al-Ti-V-Cr-$Si_{7.2}$. Failure is spotted during final casting, but during re-heating as well. Both alloys are produced utilizing Vacuum Arc Melting (VAR) technique and both were re-melted 5 times in combination with electromagnetic stirring, in order to achieve a fully homogenized microstructure. Based on the findings, the failure took place in the first 10 minutes after casting and during slow cooling and expected to be below 700°C. The same failure occurred during re-heating stage and specifically during the 3rd re-melting step.

Regarding means of fractography and metallography, fractured samples surfaces were investigated via stereoscope and scanning electron microscopy (SEM). Subsequently, sample preparation usual for microscopy observation via optical (OM) was applied. This included cutting through the transversal axis of fracture surfaces, grinding and polishing.

## 3 Results-Discussion

### 3.1 Fractography analysis of Equiatomic Al-Ti-V-Cr and Al-Ti-V-Cr-$Si_{7.2}$

In Fig. 2 macroscopic analysis it is evident the intense reflectance of the fractured surface. Generally, higher reflectance is related to coarse grain size. By means of SEM, elongated and very sharp ridges can be seen. Grain structure is not distorted and this is a typical characteristic of intergranular fractures.

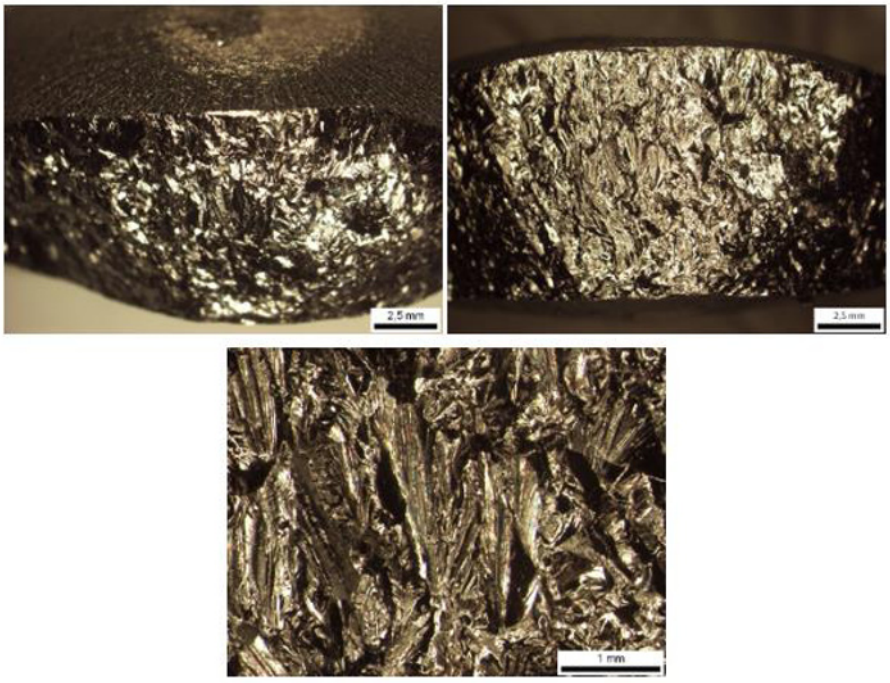


Fig. 2: Fracture surface of equiatomic Al-Ti-V-Cr.

In macroscopic scale high reflectance is still present, but in this case, it is less than before. Silicon addition leads to a grain structure as shown Fig. 3.

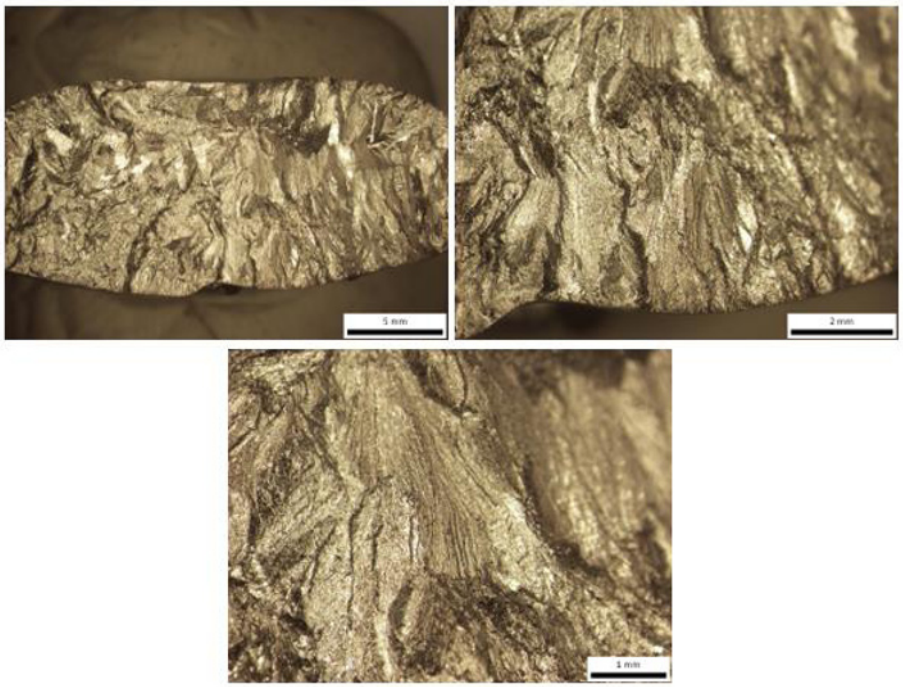


Fig. 3: Fracture surface of Al-Ti-V-Cr-$Si_{7.2}$.

By means of scanning electron microscopy, elongated and very sharp river lines/ridges can be detected. Although, grains structure is not distorted and a mixed formation of intergranular and seemingly intragranular fracture can be seen. There is no specific oriented flow and ridges seem to form, meet the pores and overlap them as shown in Fig. 4.

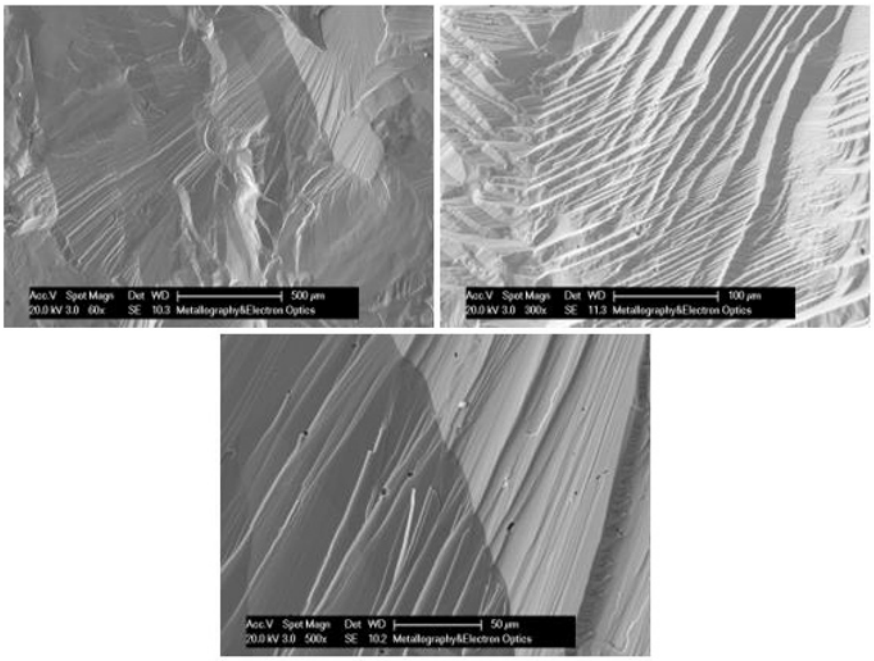


Fig. 4: Scanning electron microscopy fracture analysis of equiatomic Al-Ti-V-Cr.

In Fig. 5, the formation of elongated ridges is evident again. The phenomenon of meeting and overlaping any reported porosity is still the same. After careful examination, it is not possible to pinpoint and specific starting point of fracture and no orientation in material flow. Furthermore, no unmelted silicon particles or pure metal are found.

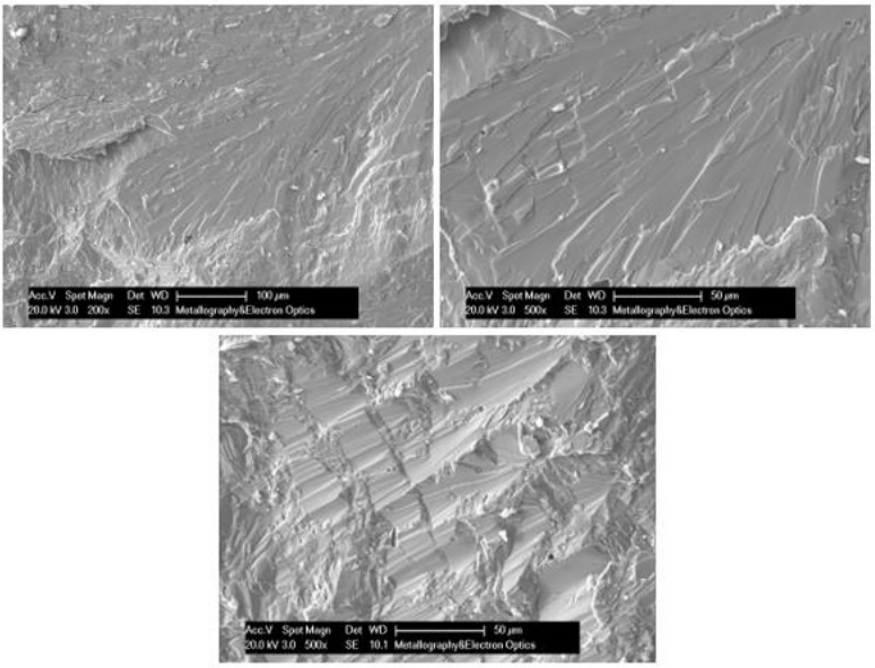


Fig. 5: Scanning electron microscopy fracture analysis of equiatomic Al-Ti-V-$Cr_{7.2}$.

### 3.2 Optical Microscopy for Equiatomic Al-Ti-V-Cr and Al-Ti-V-Cr-$Si_{7.2}$

After polishing stage, the microstructure of the equiatomic Al-Ti-V-Cr can be studied. It is consisted of coarse dendritic structure, which is stronger at upper surface and less visible at mold/sample surface, as shown in Fig. 6. Moreover, grains seem to be more equiaxed grains close to the mold/sample interface. Also, some porosity can be seen closer to the upper surface, probably due to the stirring process during the melting.

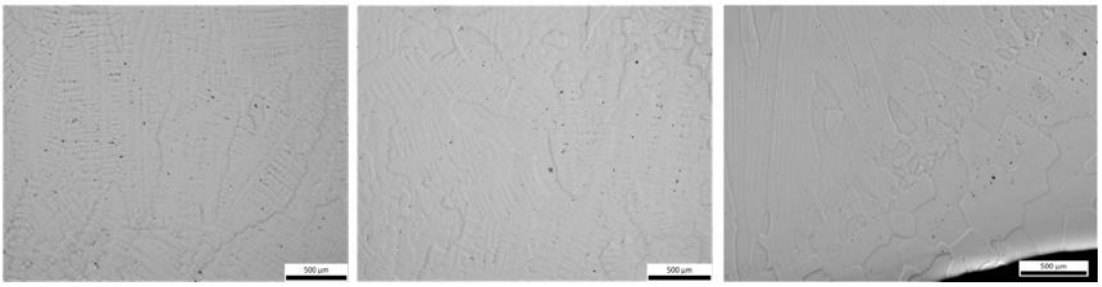

Fig. 6: Micrographs of Al-Ti-V-Cr upper surface, center and mold-sample interface (from left to right).

In the case of the microalloyed Al-Ti-V-Cr-$Si_{7.2}$ the microstructure is consisted as well of coarse dendrites (finer compared to Al-Ti-V-Cr), but with the additional formation of $Ti_5Si_3$ secondary phases. Worthy to mention is the fact that finer dendrites can be seen close to the mold/sample interface, while some porosity is still present in this alloy Fig. 7.

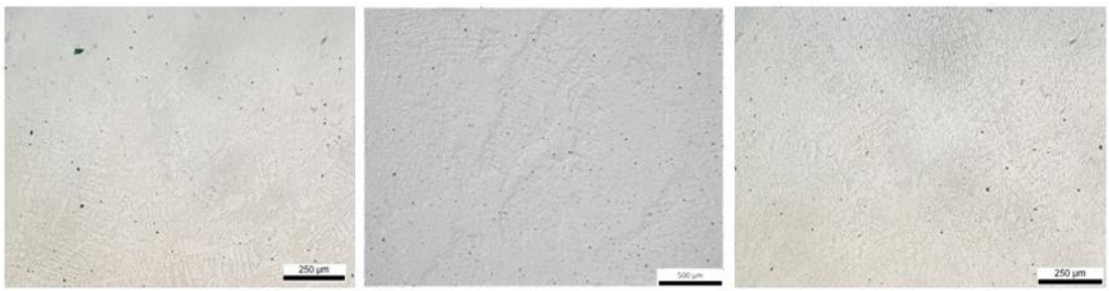

Fig. 7: Micrographs of Al-Ti-V-Cr-$Si_{7.2}$ upper surface, center and mold-sample interface (from left to right).

### 3.3 Discussion

There are various possible reasons for the failure of both alloys [11][12]. For example, insufficient melting of the selected raw materials or insufficient homogenization maybe cause abnormalities in the material, which would lead to fracture. But as it is proven above, these are not reasons for the failure. Moreover, it is possible that a reduction of ductility, due to "order-disorder" transformation, took place and the co-existence of BCC_B2 and retained BCC_A2 phase would lead to the brittle fracture. Last but not least, high Cr content may contribute to the brittle nature of those alloys.

The type of fracture seems to be a mixed mechanisms with intergranular and transgranular observations and the alloys tend to fail in a brittle manner. There was not feasible to spot a clearly visible dominant fracture mechanism and starting point. It is worthy to mention that the cooling rate is not very rapid, thus maybe faster rates would be better in order to avoid future failures. In the observed microstructure no oxides or un-melted material or inclusions

were spotted. Chemical composition is exactly the intended one and no huge deviation can be reported. In addition, the whole process was conducted under specific standards and the mold design is not a problem in this case. Porosity which is present do not act as the starting point for fracture. Regarding mechanical properties, the alloys can be characterized by low ductility. Measured hardness values are around 630 $HV_{0.2}$ for the Al-Ti-V-Cr and 760 $HV_{0.2}$ for the Al-Ti-V-Cr-$Si_{7.2}$. The fracture effect can be associated on the "order-disorder" transformation as shown from thermodynamic calculations. It is reported that "order-disorder" creates an imbalance of Young's Modulus between phases [8]. At this stage we can only speculate that this imbalance leads to unhomogenities and results to fracture.

## 4 Conclusions

As a conclusion to this work these alloys fails in an unexpected brittle manner. Fracture takes place around the ten-minute time-lapse during cooling. Based on the cooling rate, we assume that the fracture occurs close, but below the temperature point of 700°C, which is lower than the theoretical calculated "order-disorder" temperature. Therefore, it is suggested that during cooling, the transformation of parent BCC_A2 phase to BCC_B2 phase is partially complete, leading to fracture, due to imbalance of Young's Modulus between the phases. Further investigation with transmission electron microscopy (TEM) and differential calorimetry (DIC) are required to evaluate the above hypothesis and prove its validity.

## References

[1] Y. Zhang, Y. J. Zhou, J. P. Lin, G. L. Chen, and P. K. Liaw, "Solid-Solution Phase Formation Rules for Multi-component Alloys," *Adv. Eng. Mater.*, vol. 10, no. 6, pp. 534–538, Jun. 2008, doi: 10.1002/adem.200700240.

[2] Y. Qiu *et al.*, "A lightweight single-phase AlTiVCr compositionally complex alloy," *Acta Mater.*, vol. 123, pp. 115–124, Jan. 2017, doi: 10.1016/j.actamat.2016.10.037.

[3] Y. Qiu, S. Thomas, M. A. Gibson, H. L. Fraser, K. Pohl, and N. Birbilis, "Microstructure and corrosion properties of the low-density single-phase compositionally complex alloy AlTiVCr," *Corros. Sci.*, vol. 133, no. October 2017, pp. 386–396, 2018, doi: 10.1016/j.corsci.2018.01.035.

[4] A. K. Singh and A. Subramaniam, "On the formation of disordered solid solutions in multi-component alloys," *J. Alloys Compd.*, vol. 587, pp. 113–119, 2014, doi: 10.1016/j.jallcom.2013.10.133.

[5] W. Sun, X. Huang, and A. A. Luo, "Phase formations in low density high entropy alloys," *Calphad Comput. Coupling Phase Diagrams Thermochem.*, vol. 56, no. September 2016, pp. 19–28, 2017, doi: 10.1016/j.calphad.2016.11.002.

[6] V. Soni *et al.*, "Phase inversion in a two-phase, BCC+B2, refractory high entropy alloy," *Acta Mater.*, vol. 185, pp. 89–97, 2020, doi: 10.1016/j.actamat.2019.12.004.

[7] X. Huang, J. Miao, and A. A. Luo, "Lightweight AlCrTiV high-entropy alloys with dual-phase microstructure via microalloying," *J. Mater. Sci.*, vol. 54, no. 3, pp. 2271–2277, Feb. 2019, doi: 10.1007/s10853-018-2970-4.

[8] S. Laube *et al.*, "Controlling crystallographic ordering in Mo–Cr–Ti–Al high entropy alloys to enhance ductility," *J. Alloys Compd.*, vol. 823, p. 153805, 2020, doi: 10.1016/j.jallcom.2020.153805.

[9] "The Body Centered Cubic (A2) Lattice." https://www.atomic-scale-

physics.de/lattice/struk/a2.html (accessed Aug. 25, 2021).

[10] "The CsCl (B2) Structure." https://www.atomic-scale-physics.de/lattice/struk/b2.html (accessed Aug. 25, 2021).

[11] Sina Ebnesajjad, *Surface Treatment of Materials for Adhesive Bonding Surface Treatment of Materials for Adhesive Bonding*. 2014.

[12] "[PDF] Fractography: Observing, Measuring and Interpreting Fracture Surface Topography | Semantic Scholar." https://www.semanticscholar.org/paper/Fractography%3A-Observing%2C-Measuring-and-Interpreting-Hull/6aaeb7ce097bb15c9eea2dc02dfc48f7f6652af0 (accessed Aug. 25, 2021).